Simulation of a penning trap

Simon Halstensen, Carl Fredrik Nordbø Knutsen, Herman Brunborg & Didrik Sten Ingebrigtsen
(Dated: October 25, 2021)

We have investigated the resonance of particles in an idealized penning trap with a time-dependent electric potential. To accomplish this, we have run penning trap-simulations with Ca^+-ions for electric potentials with different frequencies and amplitudes. Through these simulations we find the resonance frequencies of the calcium particles in the penning trap. We proceed to run more simulations with 100 Ca^+-ions with coulomb interactions between particles for a resonance frequency. We ultimately find that the particle interactions disrupt the resonance of the Ca^+-ions in the penning trap.

I. INTRODUCTION

In this report, we are examining how particles behave in a penning trap. A penning trap is a device that applies a homogenous magnetic field and an inhomogenous electric field in an area to trap a charged particle. The penning trap can be a very useful tool for physicists, which is why we are using numerical simulations to study it.

In particular we will look at Ca^+-ions in a penning trap with a time-dependent, periodic electric potential. When applying a time-dependent force to particles, such as the force from our electric field, resonance can occur. We intend to use numerical simulations to find out under what circumstances resonance occurs in the penning trap. More concretely, we will use the algorithm Runge-Kutta 4 to solve the equations of motion of the particles numerically.

In the methods-section we will first explain the physics we use in the report. Next, we derive an analytical solution for the movement of a single particle in a penning trap with a constant electric potential, and bounds for solutions where the particles remain in the trap. We wrap up the methods-section by explaining the algorithm Runge-Kutta 4. In the results and discussion-section we first look at the performance of Runge-Kutta 4. Next, we find resonance frequencies of Ca^+-ions by simulating a penning trap with a time-dependent electric potential. We proceed to simulate 100 particles in the penning trap for a resonance frequency, both with and without coulomb interactions between particles.

II. METHODS

We model the particles being trapped inside the Penning trap with ordinary differential equations (ODEs) derived from foundational physics equations. Let us quickly go through them here, before using them to argue our model is valid. The first of these equations is Newton's second law

(1), which we use to say something about how our particles' velocity is changed in relation to outside forces. Here m is the mass of the particle, while r is its position in Euclidean space. F_i is the ith force.

$$m\ddot{r} = \sum_i F_i \tag{1}$$

Next comes the equation for how strong an electric field is at a point r, when the field is set up by point charges (2). In this equation we introduce k_e as Coulomb's constant, q as charge, and say that q_j and r_j are the jth particles' charge and position respectively.

$$E = k_e \sum_{j=1}^{n} q_j \frac{r - r_j}{|r - r_j|^3} \tag{2}$$

Electric fields (E) and potential (V) are related through (3).

$$E = -\nabla V \tag{3}$$

Lastly, the Lorentz force (4) is the force acting on a charged particle moving through an electrical and magnetic field, where the magnetic field is represented by B.

$$F = qE + qv \times B \tag{4}$$

In addition to these fundamental equations, we have two equations describing how an idealized Penning trap work, that we need to use for our model as well. The electric potential inside the trap is defined by (5), where V_0 is the potential applied at the terminals, d is the characteristic distance, a dimensionless size, and x, y and z together make up a position.

$$V(x, y, z) = \frac{V_0}{2d^2}(2z^2 - x^2 - y^2) \tag{5}$$

The magnetic field in the trap is defined as in (6). Here, B_0 is the field strength.

$$B = B_0 \hat{e}_z = (0, 0, B_0) \tag{6}$$

With these equations, we can start to model how particles would behave in proximity of or inside the trap.

Using (1) and (4), and then inserting the properties of our electrical (5) and magnetic (6) fields, we get

$$m\ddot{r} = qE + q\dot{r} \times B$$
$$0 = -m\ddot{r} + q(-\nabla V) + q\dot{r} \times B_0\hat{e}_z$$
$$0 = -m\ddot{r} + q\frac{V_0}{2d^2}\begin{pmatrix} -2x \\ -2y \\ 4z \end{pmatrix} + q\begin{pmatrix} \dot{y}B_0 \\ -\dot{x}B_0 \\ 0 \end{pmatrix}$$
$$0 = \frac{1}{m}\begin{pmatrix} \ddot{x} - qV_0x/d^2 - q\dot{y}B_0 \\ \ddot{y} - qV_0y/d^2 + q\dot{x}B_0 \\ \ddot{z} + qV_02z/d^2 \end{pmatrix}$$

If we now introduce $\omega_0 = \frac{qB_0}{m}$ and $\omega_z^2 = \frac{2qV_0}{md^2}$, and split the vector equations into separate equations, we have that

$$\ddot{x} - \omega_z^2 x/2 - \omega_0\dot{y} = 0 \tag{7}$$
$$\ddot{y} - \omega_z^2 y/2 + \omega_0\dot{x} = 0 \tag{8}$$
$$\ddot{z} + \omega_z^2 z = 0 \tag{9}$$

This is a set of three ODEs, where the two first of them are coupled. To solve them more easily, we introduce the complex function $f = x + iy$. Differentiating this twice with regards to time gives us two other equations that we can use to rewrite (7) and (8) into one complex equation.

$$\dot{f} = \dot{x} + i\dot{y}, \text{ and } \ddot{f} = \ddot{x} + i\ddot{y}.$$

We begin with (7), and insert expressions for $\ddot{x}$, $\dot{y}$ and x derived from our expression for f.

$$\ddot{x} - \omega_0\dot{y} + \frac{1}{2}\omega_z^2 x = 0$$
$$\left(\ddot{f} - i\ddot{y}\right) - \omega_0\left(\frac{\dot{f}\dot{x}}{i}\right) + \frac{1}{2}\omega_z^2\left(f - iy\right) = 0$$

We then insert an expression for $\ddot{y}$ derived from f, and get

$$\ddot{f} - i\left(-\omega_0\dot{x} + \frac{1}{2}\omega_z^2 y\right) + i\omega_0\dot{f}\dot{x} + \frac{1}{2}\omega_z^2\left(f - iy\right) = 0$$
$$\ddot{f} + i\omega_0\dot{x} - \omega_0\dot{x} + \frac{1}{2}\omega_z^2 iy - \frac{1}{2}\omega_z^2 iy + i\omega_0\dot{f} - \frac{1}{2}\omega_z^2 f = 0$$
$$\ddot{f} + i\omega_0\dot{f} - \frac{1}{2}\omega_z^2 f = 0$$

We now have two ODEs that together describe how particles behave in and around our trap. $\ddot{f} + i\omega_0\dot{f} - 1/2\omega_z^2 f = 0$ gives us information about the x-axis (Re(f)) and y-axis (Im(f)), and $\ddot{z} + \omega_z^2 z = 0$ describes the movement along the z-axis.

Let us now analyse how our model predicts the particles will behave in the xy-plane. The analytical solution of our complex ODE is

$$f(t) = A_+e^{-\omega_+ t} + A_-e^{-\omega_- t}, \tag{10}$$

where

$$\omega_\pm = \frac{\omega_0 \pm \sqrt{\omega_0^2 - 2\omega_z^2}}{2},$$

and $A_\pm$ are constants set after inserting initial conditions.

If we want to trap the particles, we want $|f(t)| < \infty$ even when $t \to \infty$. This means the real component of the exponent must be non-positive, in other words Re$(-i\omega_\pm) \leq 0$. It could also be that only one of our two terms have non-positive exponents, and A associated with the other term is 0, but this is highly dependent on initial conditions, and thus very unstable. To understand the relationship between our trap's parameters (B_0, V_0 and d) and the particle's properties (q and m), let us expand our $\omega_\pm$-expression and solve the resulting equation.

$$0 \geq \text{Re}\left(-i\omega_\pm\right)$$
$$= \text{Im}\left(-\omega_\pm\right)$$
$$= \frac{1}{2}\text{Im}\left(-\omega_0 \mp \sqrt{\omega_0^2 - 2\omega_z^2}\right)$$
$$= \text{Im}\left(-\omega_0\right) + \text{Im}\left(\mp\sqrt{\omega_0^2 - 2\omega_z^2}\right)$$
$$= \mp\text{Im}\left(\sqrt{\omega_0^2 - 2\omega_z^2}\right).$$

This means the imaginary component of the square root must have a strict equality with 0, which only happens if $\omega_0^2 - 2\omega_z^2 > 0$, meaning that we get

$$\frac{4V_0}{d^2 B_0^2} < \frac{q}{m},$$

if we insert our expressions for ω_0 and ω_z^2. This last equation gives us some opportunity to interpret how the particle should behave. The key insight it provides is that the higher the charge of the particle, and lower mass it has, the higher the potential applied to the terminals can be without it pushing the particle out of the trap in the xy-plane.

The fact that the real component of the exponents has to be 0 also lets us know something about the upper and lower bounds for the distance the particles can have from the origin in the xy-plane. Breaking up the motion of the particles in to $f(t) = g(t) + h(t)$, where $g(t) = A_+e^{i\omega_+ t}$ and $h(t) = A_-e^{i\omega_- t}$, we have that $|g(t)| = |A_+|$ and $|h(t)| = |A_-|$ for all t. In other words, g and h describe circular motion in the complex plane, with radii $|A_+|$ and $|A_-|$ respectively, and center in the origin. Then the argument for finding upper and lower bounds on the distance to the origin is a simple geometric one. We get the upper bound R_+ if $\text{Arg}(g(t)) = \text{Arg}(h(t))$, i.e when $g(t)$ and $h(t)$ contributes in the same direction. Then clearly $|f(t)| = ||A_+| + |A_-||$, meaning $R_+ = |A_+| + |A_-|$. We get our lower bound if $g(t)$ and $h(t)$ contributes in opposite directions. Then $|f(t)| = ||A_+| - |A_-||$, so $R_- = ||A_+| - |A_-||$.

THE ALGORITHM

In this project we will be using Runge-Kutta 4 to solve our ODE's on the time-interval $[0, T]$, for n intervals of length h. Runge-Kutta 4 is a fourth order Runge-Kutta method with an error of $\epsilon = \mathcal{O}(h^4)$. It is a general method for solving ODE's, but here we will adapt the algorithm to solve the equations of motion when an expression $a(r, t)$ for the acceleration is known from 1. Assuming that you know the initial position r_0 and initial velocity $\dot{r}_0 = v_0$ of a particle, we can approximate and discretise the differential equation with Runge-Kutta 4. To numerically solve the equations such that $r_i \approx r(ih)$ and $v_i \approx v(ih)$ for $i \in \{0, 1, 2, \ldots, n\}$, we use algorithm 1.

Algorithm 1 Runge-Kutta 4 for solving equations of motion

1: $r_0 \leftarrow r(0)$
2: $v_0 \leftarrow v(0)$
3: $n \leftarrow \dfrac{T}{h}$
4: **for** $i \in \{0, 1, 2, \ldots, n - 1\}$ **do**
5:     $K_{1,v} \leftarrow a(r_i, t_i)$
6:     $K_{1,r} \leftarrow v_i$
7:     $K_{2,v} \leftarrow a(r_i + \dfrac{h}{2}K_{1,v}, t_i + \dfrac{h}{2})$
8:     $K_{2,r} \leftarrow v_i + \dfrac{h}{2}K_{1,r}$
9:     $K_{3,v} \leftarrow a(r_i + \dfrac{h}{2}K_{2,v}, t_i + \dfrac{h}{2})$
10:     $K_{3,r} \leftarrow v_i + \dfrac{h}{2}K_{2,v}$
11:     $K_{4,v} \leftarrow a(r_i + hK_{3,v}, t_i + h)$
12:     $K_{4,r} \leftarrow v_i + hK_{3,r}$
13:     $v_{i+1} = \dfrac{h}{6}(K_{1,v} + 2K_{2,v} + 2K_{3,v} + K_{4,v})$
14:     $r_{i+1} = \dfrac{h}{6}(K_{1,r} + 2K_{2,r} + 2K_{3,r} + K_{4,r})$
    return v, r

In reality, the code may be slightly more complex than what is found in algorithm 1 as multiple particles are able to interact with each other.

Before looking for resonance in our penning trap, we test our implementation of Runge-Kutta against the analytical solution (Appendix V) and against the simpler Forward Euler method. We also use the result from here to decide on a reasonable step size h in the simulation. In doing this, we provide some insight to the error convergence rate r_{err} of the two methods.

$$r_{\mathrm{err}} = \frac{1}{4} \sum_{k=2}^{5} \frac{\log(\Delta_{\mathrm{max},k}/\Delta_{\mathrm{max},k-1})}{\log(h_k/h_{k-1})}$$

with $\Delta_{\mathrm{max},k} = \max_i |r_i - r_{i,\mathrm{exact}}|$

It's useful to be able to turn off coulomb interactions, so we experiment with this feature, making sure it's implemented correctly.

III. RESULTS AND DISCUSSION

Simulation of particle position for $p_0 = (100, 0, 100)$, $v_0 = (0, 1, 0)$, $\Delta t = 10^{-3}$, $N = 10^5$
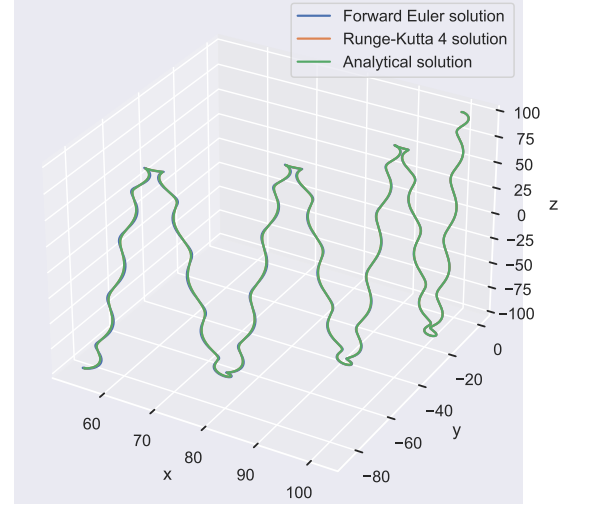

FIG. 1. The position of the particle as according to the analytical solution, a Forward Euler simulation and a Runge-Kutta 4 simulation

Simulating the penning trap with Runge-Kutta 4 gives output that follows the analytical solution very closely. In comparison we observe some very small deviation in the solution from Forward Euler (FIG. 1).

Figure (2) more closely analyzes the error of our simulation. Here we show the relative error using 5 different step sizes and $t \in [0, 100]\mu s$. In figure (3) we do the same for Forward Euler. Using this we get to say something about the rate of convergence for Runge-Kutta 4 and Forward Euler. For Forward Euler we estimate $r_{\mathrm{err}} = 0.811$, while Runge-Kutta 4 as expected performs better at $r_{\mathrm{err}} = 1.93$. While this is significantly lower than the expected $\mathcal{O}(h^4)$, this might be because this is a poor estimate. This might have something to do with the anomalies we see in figure (2).

We clearly see from our results that the step size affect the precision of the simulation, with smaller step sizes giving solutions closer to the analytic one. When deciding on a step size for finding resonance, precision is obviously a concern. However smaller step sizes also gives more computationally heavy simulations. With this in mind, we decided on a step size of $h = 10^{-2}$.

It's also worth noting that the error grows as t grows. This is important as we are about to look at the state of the penning trap $500\mu s$ in.

Figure (4) shows the effect of turning off the coulomb interactions, as a plot of the path in the xy-plane. Figure (5) also shows the effect of turning off the interactions,

with a 3D-plot of the trajectories of the particles. As expected, turning off coulomb interactions slightly alters the path of the particle. Importantly, turning off coulomb interactions greatly reduces the time it takes to carry out the simulations. This means we can simulate many more particles, as we need to when looking for resonance.

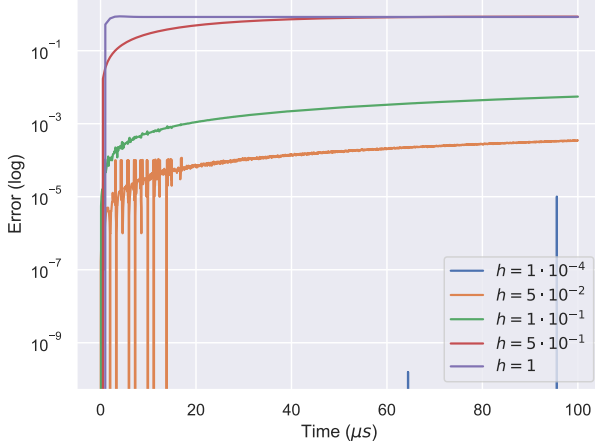Relative error of Runge Kutta 4

FIG. 2. The relative error for the Runge-Kutta 4 method as compared to the analytical solution

Relative error of Forward Euler
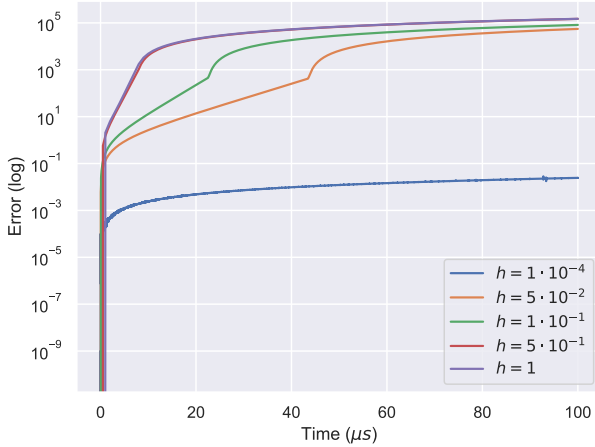
FIG. 3. The relative error for the Forward Euler method as compared to the analytical solution

For a time-dependent electric field we repeated simulations of 100 Ca^+-ions with amplitudes $f = 0.1, 0.4, 0.7$, without coulomb interactions. We did the simulations for evenly spaced frequencies ω_V in the interval $[0.2, 2.5]$MHz, and counted the number of particles left in the penning trap after $500\mu s$ for a step size $h = 10^{-2}$.

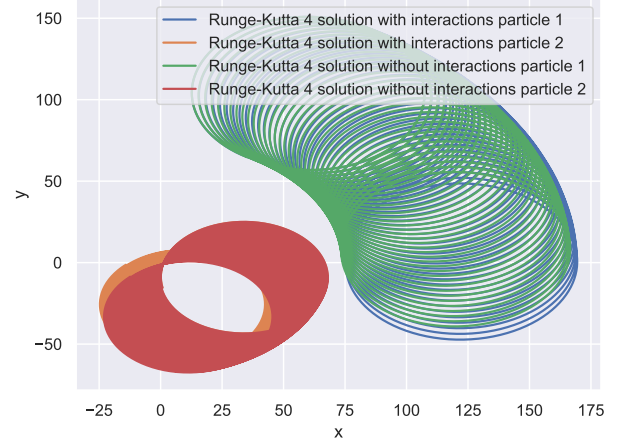Motion of two particles in the xy-plane with and without coulomb interaction

FIG. 4. The simulations of two particles with and without coulomb interactions

Motion of two particles in the xy-plane with and without interaction in 3D
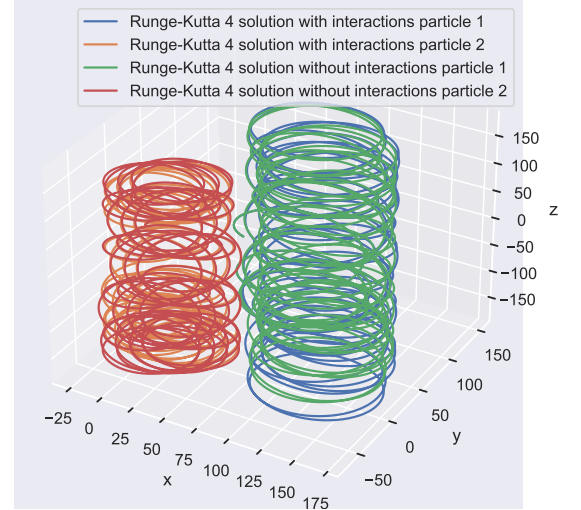

FIG. 5. The simulations of two particles with and without coulomb interactions in 3d

Figure (6) shows that for all of the amplitudes tested there is a significant lowering of the number of particles left in the trap when the frequency is $\omega_V \approx 0.44$MHz. We also can see a clear lowering of particles left for $\omega_V \approx 0.22$MHz for $f = 0.7$.

The fact that the resonance frequency at 0.22 is half of the resonance frequency 0.44 is a reasonable result. In general if $\omega_{V,0}$ is the fundamental frequency, the highest resonance frequency, then $\dfrac{\omega_{V,0}}{2}, \dfrac{\omega_{V,0}}{3}, \dfrac{\omega_{V,0}}{4} \cdots$ are all resonance frequencies. In our case, 0.44 appears to be our fundamental frequency, which fits with our
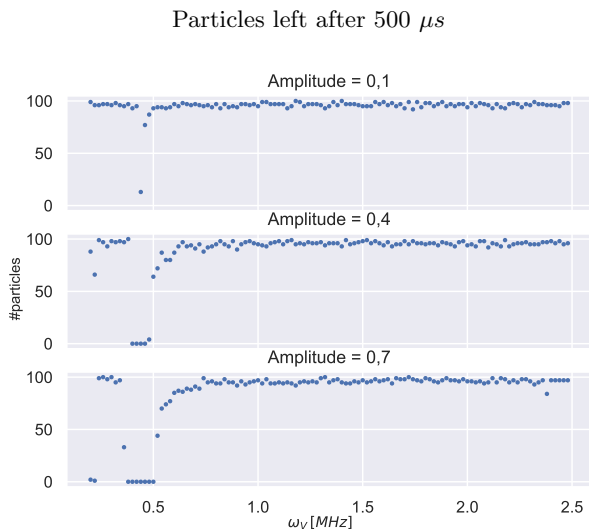
Particles left after 500 μs

FIG. 6. Particles left in the penning trap for different frequencies

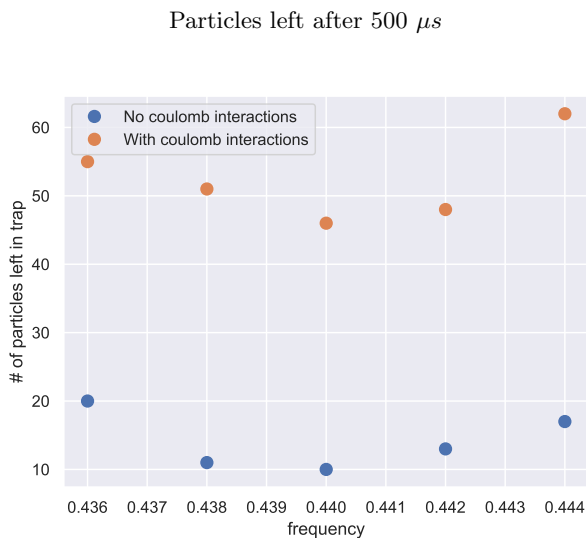Particles left after 500 μs

FIG. 7. Particles left in the penning trap for different frequencies with and w/o coulomb interactions

finding that $\dfrac{0.44}{2}$ is also a resonance frequency.

As the external electric force is a periodic, time-dependent force, it is natural to explain the behavior of the particles with resonance. If a calcium ion has a resonance frequency equal to the frequency ω_V of the electric field, the oscillation of the particle is amplified. This is seemingly what is happening in our simulations. If the frequency of the electric field is close to a resonance frequency of the calcium ions, the particles' oscillations increase in amplitude. This can in turn lead to the particles moving outside of the penning trap, which is why certain frequencies ω_V lead to a large amount of particles leaving the trap.

We can also see that the breadth of the interval of frequencies where the particles all leave the trap increases as the magnitude of the electric field oscillation increases. As the magnitude increases, the oscillations become bigger.

Next, we proceeded to do a more fine-grained simulation for $f = 0.1$, both with and without coulomb interactions around $\omega_V = 0.44$MHz. We tested with 5 evenly spaced values of ω_V in the interval $[0.436, 0.444]$MHz. As figure (7) shows, it seems we have a local minimum for the numbers of particles left after $500\mu s$ at around 0.44MHz.

From figure (7) it also seems we observe less resonance when accounting for the interactions between particles. This suggests that the particles' interactions disrupt the resonant oscillation that we observed without particle interactions. This result seems reasonable, as resonance occurs when a periodic force coincides with periodic movement. When coulomb interactions with 99 other particles unpredictably affects the movement of a particle, the movement is no longer perfectly periodic. Therefore it makes sense that there occurs less resonance.

IV. CONCLUSION

The first part of the results suggests that we can trust our implementation of Runge-Kutta 4, but that the hardware limitations we are working with might have meant that the results weren't as accurate as they needed to be. We analyzed the system a full $500\mu s$ in, which meant we would need a very accurate simulation to be able to trust the result at the end.

We are nevertheless satisfied with having observed resonance in our penning trap, and having found how the amplitude of the time-dependent potential interacts with this. Also seeing that accounting for coulomb interactions disrupts the resonance phenomena was interesting.

We have some suggestions for further work that could give additional insight into resonance phenomena inside idealized penning traps. In particular, it could be informative to further investigate the conditions that allow us to observe resonance in the penning trap. One could for instance repeat simulations with different amounts of particles to describe the relation between the number of particles and resonance. One could also run fine-grained scans, for frequencies $\omega_V = \dfrac{0.44}{2}, \dfrac{0.44}{3}, \dfrac{0.44}{4}, \dots$ to check that these are resonance frequencies.

Addit, we would want to optimize and parallelize the source code, so we could realistically run the

simulations with a smaller step size.

V. APPENDIX

CODE

The code used to produce the plots is available at https://github.com/hermanbrunborg/FYS4150-Project-3

Appendix i

To test our implementation, we want to find a specific analytical solution given some initial conditions, and compare this with what our numerical approach gives us. Let us therefore assume we have a single charges particle in our Penning trap, with

$$x(0) = x_0, \quad \dot{x}(0) = 0, \quad y(0) = 0, \quad \dot{y}(0) = v_0,$$
$$z(0) = z_0, \text{ and } \dot{z}(0) = 0.$$

Next, we use our general analytical solution for the xy-plane (eq 10) to find a specific solution given the initial conditions listed above. We then get two equations

$$A_+ e^0 + A_- e^0 = x_0 \tag{11}$$
$$-i\omega_+ A_+ e^0 - i\omega_- A_- e^0 = v_0 i, \tag{12}$$

which we can write as the matrix equation

$$\begin{pmatrix} 1 & 1 & x_0 \\ -i\omega_+ & -i\omega_- & v_0 i \end{pmatrix} \sim \begin{pmatrix} 1 & 0 & \frac{v_0 + x_0\omega_-}{\omega_- - \omega_+} \\ 0 & 1 & -\frac{v_0 + x_0\omega_+}{\omega_- - \omega_+} \end{pmatrix}.$$

This means that our specific solution in the xy-plane has

$$A_+ = \frac{v_0 + x_0\omega_-}{\omega_- - \omega_+} \quad A_- = -\frac{v_0 + x_0\omega_+}{\omega_- - \omega_+}.$$

We then find the general analytical solution for the z-axis by finding the characteristic equation of (9), which is $r^2 + \omega_z^2$, implying $r = \pm\omega_z i$. An ODE of this type, with a characteristic equation with two imaginary roots, has the general form

$$z(t) = C_1 \sin t + C_2 \cos t.$$

With our initial conditions, this becomes

$$z(t) = z_0 \cos t.$$

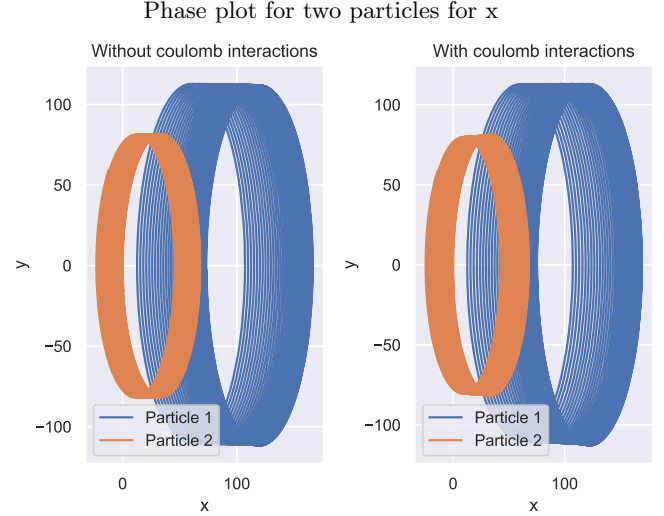We use the specific analytical solutions above to test that our numerical implementations work properly.
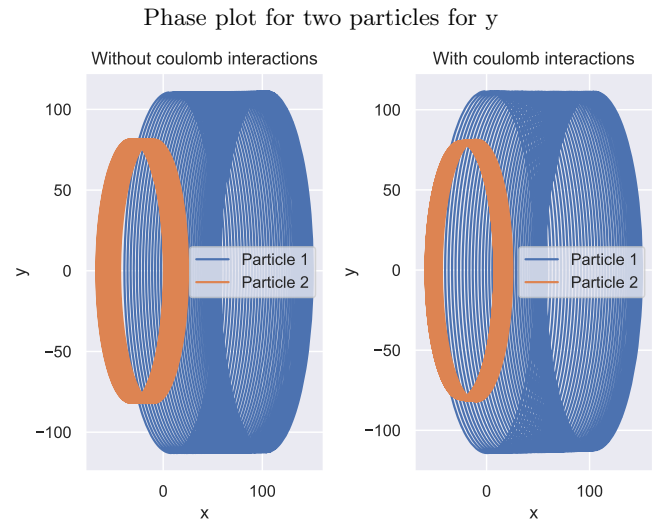
Appendix ii

Phase plot for two particles for x

FIG. 8. The phase plot for the particles in x-direction

Phase plot for two particles for y

FIG. 9. The phase plot for the particles in x-direction

Phase plot for two particles for z

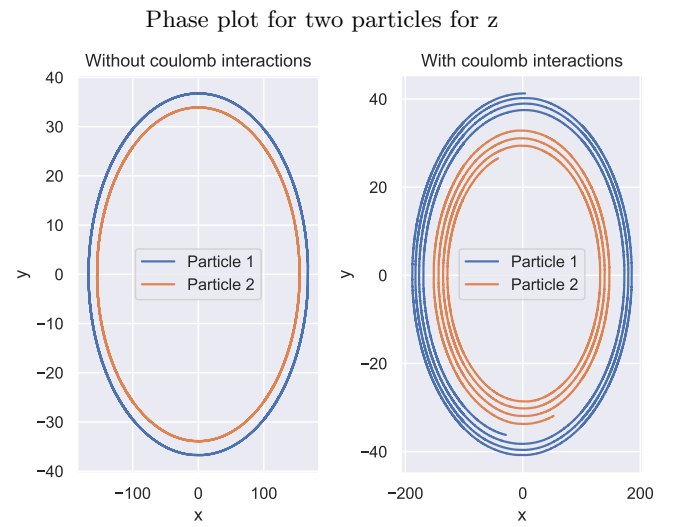

FIG. 10. The phase plot for the particles in x-direction

References

[1] Nave R. (2009) Fundamental and Harmonics. Retrived from http://hyperphysics.phy-astr.gsu.edu/hbase/Waves/funhar.html 25th of October 2021